

Thermal destabilization of self-bound ultradilute quantum droplets

Jia Wang, Hui Hu, and Xia-Ji Liu

Centre for Quantum Technology Theory, Swinburne University of Technology, Melbourne, Victoria 3122, Australia

(Dated: July 7, 2020)

We theoretically investigate the temperature effect in a Bose-Bose mixture with attractive inter-species interactions, in the regime where a self-bound ultradilute quantum droplet forms due to the subtle balance between the attractive mean-field force and the repulsive force provided by Lee-Huang-Yang quantum fluctuations. We find that in contrast to quantum fluctuations, thermal fluctuations destabilize the droplet state and completely destroy it above a threshold temperature. We show that the threshold temperature is determined by the intra-species interaction energy. For a three-dimensional Bose-Bose mixture, the threshold temperature is less than one-tenth of the Bose-Einstein condensation temperature under the typical experimental conditions. With increasing temperature, the droplet's equilibrium density gradually decreases and can be reduced by several tens of percent upon reaching the threshold temperature. We also consider a one-dimensional quantum droplet and find a similar destabilization effect due to thermal fluctuations. The threshold temperature in one dimension is roughly set by the binding energy of the inter-species dimer. The pronounced thermal instability of a self-bound quantum droplet predicted in our work could be examined in future experiments, by measuring the temperature dependence of its central density and observing its sudden disappearance at the threshold temperature.

I. INTRODUCTION

In his classical textbook “*The Universe in a Helium Droplet*” [1], Volovik described an interesting autonomously isolated quantum system of helium nanodroplet, without any interaction with the surrounding environment. It can be in equilibrium at *zero* external pressure (i.e., $P = 0$) in empty space, with an equilibrium particle density $n_{\text{eq}} \sim 2 \times 10^{22} \text{cm}^{-3}$ [2–4] determined by the balance between the attractive interatomic interaction ($\propto n$) and the repulsive zero-point quantum motions of helium atoms ($\propto n^{3/2}$). As a *negative* chemical potential $\mu < 0$ is needed to prevent self-evaporation, the droplet formation is generally impossible in the well-studied single-component weakly interacting Bose gas of ultracold alkali-metal atoms [5], where the attractive short-range inter-particle interactions lead to a mean-field collapse [6].

The situation, however, can dramatically change if one considers a binary Bose mixture with both short-range attractive inter-species interactions ($g_{12} < 0$) and repulsive intra-species interactions ($g > 0$), as suggested by Petrov in his seminal work [7]. When $g_{12} < -g$, although the mean-field theory predicts a collapsing state, the inclusion of Lee-Huang-Yang (LHY) quantum fluctuations [8] (i.e., the zero-point oscillations) turns out to stabilize the mechanical collapse and leads to the formation of an ultradilute droplet at equilibrium density $n_{\text{eq}} \sim 10^{14} \text{cm}^{-3}$, which is about eight orders of magnitude more dilute than a liquid ^4He droplet. Petrov's ground-breaking idea has now been successfully confirmed experimentally with homonuclear ^{39}K - ^{39}K mixtures [9–12] and heteronuclear ^{41}K - ^{87}Rb mixtures [13]. Ultradilute quantum droplets have also been observed in scalar weakly-interacting Bose gases with anisotropic long-range dipolar interactions [14–17], following more closely the picture by Volovik. These rapid experimen-

tal developments open a new fast-moving research direction, where several intriguing many-body effects can be predicted theoretically [18–34] and examined experimentally [9–17], beyond the existing paradigm of helium nanodroplets [2–4].

In this work, we would like to understand how quantum droplets' *bulk* properties are affected by a small but nonzero temperature, which always exists experimentally. This issue is rarely addressed in the past literature, presumably due to the lack of a useful microscopic theory of quantum droplets from the first principle. Here, we overcome such a difficulty by extending a most recently developed pairing description of the droplet state [35–37] to finite temperatures. For simplicity, we follow Petrov's binary Bose mixture model of quantum droplets [7], to avoid subtly treating the long-range anisotropic dipolar interactions in dipolar droplets.

We find that thermal fluctuations generally destabilize the droplet. This tendency is natural to understand. As temperature increases, the atomic motion becomes increasingly significant, and the droplet may fail to maintain its zero-pressure state. We observe that the threshold temperature for the complete destruction of the quantum droplet is typically set by the intra-species interaction energy. For a weakly interacting Bose-Bose mixture in three dimensions, the interaction energy is small, so the threshold temperature could be less than one-tenth of the condensation temperature under the current experimental conditions [9, 11]. Remarkably, despite this low threshold temperature, the equations of state of quantum droplets still show a strong temperature dependence. In particular, with increasing temperature, the droplet's equilibrium density can be reduced by several tens of percent upon reaching the threshold temperature. We also consider the droplet state in a Bose-Bose mixture in one dimension and find similar thermal destabilization due to thermal fluctuations.

The rest of the paper is organized as follows. In the next section (Sec. II), we introduce the model Hamiltonian and present a microscopic pairing theory of quantum droplets at low but finite temperature based on the conventional Bogoliubov theory [38]. In Sec. III, we discuss the thermal destabilization of quantum droplets in three dimensions. The quantum depletion and thermal depletion are calculated to validate the applicability of the Bogoliubov theory. In Sec. IV, we consider one-dimensional quantum droplets and show that the thermal destabilization effect is universal for the droplet state in different dimensions. Finally, Sec. V is devoted to the conclusions and outlooks.

II. PAIRING THEORY AT FINITE TEMPERATURE

To highlight the essential temperature effect, we consider the *simplest* possible homonuclear Bose-Bose mixture, with equal repulsive intra-species interactions (i.e., $g_{11} = g_{22} = g$) and attractive inter-species interactions (g_{12}). In this case, we have equal population in each species and equal chemical potential μ . In real space, the system is described by a grand canonical model Hamiltonian, $\hat{K} = \int d\mathbf{x}[\mathcal{H} + \mathcal{H}_{\text{intra}} + \mathcal{H}_{\text{inter}}]$, with

$$\mathcal{H}_0 = \sum_{i=1,2} \hat{\phi}_i^\dagger(\mathbf{x}) \left[-\frac{\hbar^2 \nabla^2}{2m} - \mu \right] \hat{\phi}_i(\mathbf{x}), \quad (1)$$

$$\mathcal{H}_{\text{intra}} = \frac{g}{2} \sum_{i=1,2} \hat{\phi}_i^\dagger(\mathbf{x}) \hat{\phi}_i^\dagger(\mathbf{x}) \hat{\phi}_i(\mathbf{x}) \hat{\phi}_i(\mathbf{x}), \quad (2)$$

$$\mathcal{H}_{\text{inter}} = -\frac{\hat{\Delta}^\dagger \hat{\Delta}}{g_{12}} - \left[\hat{\Delta} \hat{\phi}_1^\dagger(\mathbf{x}) \hat{\phi}_2^\dagger(\mathbf{x}) + \text{H.c.} \right], \quad (3)$$

where in the last Hamiltonian density for inter-species interactions, we have used the Hubbard-Stratonovich transformation to decouple the four-fermion interaction term through the introduction of a pairing field $\hat{\Delta}(\mathbf{x})$ [36, 37]. $\hat{\phi}_i(\mathbf{x})$ and $\hat{\phi}_i^\dagger(\mathbf{x})$ ($i = 1, 2$) are annihilation and creation field operators for the i -species bosons with mass $m_1 = m_2 = m$.

In this work, we consider both three-dimensional and one-dimensional binary mixtures. In three dimensions, the short-range *contact* inter-particle interactions used in the model Hamiltonian are unphysical in the large-momentum and high-energy limit, as reflected by the well-known ultraviolet divergence. The divergence can be removed by the standard regularization procedure: we simply re-express the bare interaction strengths g_{ij} in terms of the s -wave scattering lengths a_{ij} , i.e.,

$$\frac{1}{g_{ij}} = \frac{m}{4\pi\hbar^2 a_{ij}} - \frac{1}{\mathcal{V}} \sum_{\mathbf{k}} \frac{m}{\hbar^2 \mathbf{k}^2}, \quad (4)$$

where \mathcal{V} is the volume of the system (or the length of the system in the one-dimensional case). The interaction regularization is not required in one dimension. There,

the interaction strengths g_{ij} are related to the s -wave scattering length via

$$g_{ij} = -\frac{2\hbar^2}{ma_{ij}}. \quad (5)$$

A. Bogoliubov theory with pairing

The pairing theory of quantum droplets in a binary Bose mixture has been discussed in detail in the previous works [35–37]. Here, for self-containedness we briefly review the theory and extend it to the finite temperature case. In the weakly interacting regime, we take the Bogoliubov approximation to rewrite the bosonic field operators [38–40],

$$\hat{\phi}_i(\mathbf{x}) = \phi_c(\mathbf{x}) + \delta\hat{\phi}_i(\mathbf{x}), \quad (6)$$

where $\delta\hat{\phi}_i$ is considered as small fluctuation around the condensate wave-function $\phi_c(\mathbf{x})$. At the same level of approximation, we also take a static c -number function for the pairing field [35–37], i.e.,

$$\hat{\Delta}(\mathbf{x}) = \Delta(\mathbf{x}), \quad (7)$$

and determine it *variationally*. As we focus on the ground state, both the condensate wave-function $\phi_c(\mathbf{x})$ and the pairing function $\Delta(\mathbf{x})$ can be chosen as real and non-negative functions. By expanding the model Hamiltonian in terms of $\delta\hat{\phi}_i^\dagger$ and $\delta\hat{\phi}_i$ and truncate it to the second order, we find that a quadratic form,

$$\hat{K}_B = \sum_{i=1,2} \int d\mathbf{x} \left[\delta\hat{\phi}_i^\dagger \mathcal{L} \delta\hat{\phi}_i + \left(\frac{C}{2} \delta\hat{\phi}_i^\dagger \delta\hat{\phi}_i + \text{H.c.} \right) \right] - \int d\mathbf{x} \left[\left(\Delta \delta\hat{\phi}_1^\dagger \delta\hat{\phi}_2^\dagger + \text{H.c.} \right) + \frac{C^2}{g} + \frac{\Delta^2}{g_{12}} \right], \quad (8)$$

provided that $\phi_c(\mathbf{x})$ and $\Delta(\mathbf{x})$ satisfy a Gross-Pitaevskii (GP) equation,

$$\left[-\frac{\hbar^2 \nabla^2}{2m} - \mu + C(\mathbf{x}) - \Delta(\mathbf{x}) \right] \phi_c(x) = 0, \quad (9)$$

where we have defined the short-hand notations,

$$C(\mathbf{x}) \equiv g\phi_c^2(\mathbf{x}), \quad (10)$$

$$\mathcal{L} \equiv -\frac{\hbar^2 \nabla^2}{2m} - \mu + 2C(\mathbf{x}). \quad (11)$$

The function $C(\mathbf{x})$ can be simply viewed as the intra-species interaction energy density. The quadratic form of the model Hamiltonian is straightforward to diagonalize, by a linear real-space Bogoliubov transformation [39, 40],

$$\delta\hat{\phi}_i(\mathbf{x}) = \sum_n [u_{ni}(\mathbf{x}) \hat{\alpha}_n + v_{ni}^*(\mathbf{x}) \hat{\alpha}_n^\dagger], \quad (12)$$

$$\delta\hat{\phi}_i^\dagger(\mathbf{x}) = \sum_n [u_{ni}^*(\mathbf{x}) \hat{\alpha}_n^\dagger + v_{ni}(\mathbf{x}) \hat{\alpha}_n], \quad (13)$$

where $\hat{\alpha}_n^\dagger$ and $\hat{\alpha}_n$ are creation and annihilation field operators of Bogoliubov quasiparticles, and $u_{ni}(\mathbf{x})$ and $v_{ni}(\mathbf{x})$ are the corresponding quasiparticle wave-functions. The truncated Bogoliubov Hamiltonian then becomes [37],

$$\hat{K}_B = \Omega_0 + \sum_n E_n \hat{\alpha}_n^\dagger \hat{\alpha}_n, \quad (14)$$

$$\Omega_0 = - \int d\mathbf{x} \left[\frac{C^2}{g} + \frac{\Delta^2}{g_{12}} + \sum_{ni} E_n |v_{ni}(\mathbf{x})|^2 \right], \quad (15)$$

if $u_{ni}(\mathbf{x})$ and $v_{ni}(\mathbf{x})$ obey the Bogoliubov equations,

$$\mathcal{L}u_{ni} + C(\mathbf{x})v_{ni} - \Delta(\mathbf{x})v_{n,3-i} = +E_n u_{ni}, \quad (16)$$

$$\mathcal{L}^*v_{ni} + C(\mathbf{x})u_{ni} - \Delta^*(\mathbf{x})u_{n,3-i} = -E_n v_{ni}, \quad (17)$$

where $E_n \geq 0$ is the energy of Bogoliubov quasi-particles. It is easy to check that the zero-mode with $E = 0$ has the form $u_1 = u_2 = +\phi_c(\mathbf{x})$ and $v_1 = v_2 = -\phi_c(\mathbf{x})$, which is precisely the condensate mode of the GP equation and hence should be excluded. From the diagonalized Hamiltonian (14), it is straightforward to write down the thermodynamic potential at *finite* temperature ($\beta = 1/k_B T$),

$$\Omega = \Omega_0 + \frac{1}{\beta} \sum_n \ln [1 - \exp(-\beta E_n)], \quad (18)$$

from which, we determine the variational pairing function $\Delta(\mathbf{x})$ through the *functional* minimization, i.e.,

$$\frac{\delta \Omega [\mu, \Delta(\mathbf{x})]}{\delta \Delta(\mathbf{x})} = 0. \quad (19)$$

Once $\Delta(\mathbf{x})$ is found, we calculate the total number of atoms, $N = -\partial \Omega / \partial \mu$, and consequently the free energy $F = \Omega + \mu N$. In the thermodynamic limit, the free energy per particle takes a global minimum as a function of the density $n = N/V$ when the system is in the self-bound droplet state, i.e., $\partial(F/N)/\partial n = 0$, which is equivalent to the zero-pressure condition,

$$P = -\frac{\Omega}{V} = \frac{n^2}{V} \frac{\partial(F/N)}{\partial n} = 0. \quad (20)$$

It is worth noting that the above Bogoliubov theory is applicable at low temperatures, where the depletion from the condensate, due to either quantum fluctuations or thermal fluctuations, should be sufficiently small. For this purpose, one may need to explicitly examine the quantum depletion N_{qd} and thermal depletion N_{th} . These two quantities can be evaluated by taking the average of the number operators ($i = 1, 2$),

$$\langle \delta \hat{\phi}_i^\dagger \delta \hat{\phi}_i \rangle = \sum_n \left[|v_{ni}|^2 + (|u_{ni}|^2 + |v_{ni}|^2) \langle \hat{\alpha}_n^\dagger \hat{\alpha}_n \rangle \right], \quad (21)$$

and we obtain,

$$N_{\text{qd}} = \int d\mathbf{x} \sum_{ni} |v_{ni}(\mathbf{x})|^2, \quad (22)$$

$$N_{\text{th}} = \int d\mathbf{x} \sum_{ni} \left[|u_{ni}(\mathbf{x})|^2 + |v_{ni}(\mathbf{x})|^2 \right] f_B(E_n), \quad (23)$$

where $f_B(E) = 1/(e^{\beta E} - 1)$ is the Bose-Einstein distribution function.

B. Bulk properties of quantum droplets in the thermodynamic limit

For simplicity, in this work we consider a sufficiently large droplet, where the edge effect can be safely neglected. We therefore have *constant* condensate wave-function ϕ_c , intra-species interaction energy C , and pairing parameter Δ . The GP equation (9) then leads to the relation $C = \mu + \Delta$. In this case, the quasi-particle wave-functions, $u_{\mathbf{k}i}(\mathbf{x}) = u_{\mathbf{k}i} e^{i\mathbf{k}\cdot\mathbf{x}}/\sqrt{V}$ and $v_{\mathbf{k}i}(\mathbf{x}) = v_{\mathbf{k}i} e^{i\mathbf{k}\cdot\mathbf{x}}/\sqrt{V}$, are plane waves with momentum \mathbf{k} and energy $E_{\mathbf{k}}$. The Bogoliubov equations (16) and (17) in momentum space take the form,

$$\begin{bmatrix} B_{\mathbf{k}} & 0 & C & -\Delta \\ 0 & B_{\mathbf{k}} & -\Delta & C \\ C & -\Delta & B_{\mathbf{k}} & 0 \\ -\Delta & C & 0 & B_{\mathbf{k}} \end{bmatrix} \begin{bmatrix} u_{\mathbf{k}1} \\ u_{\mathbf{k}2} \\ v_{\mathbf{k}1} \\ v_{\mathbf{k}2} \end{bmatrix} = E_{\mathbf{k}} \begin{bmatrix} +u_{\mathbf{k}1} \\ +u_{\mathbf{k}2} \\ -v_{\mathbf{k}1} \\ -v_{\mathbf{k}2} \end{bmatrix}, \quad (24)$$

where $B_{\mathbf{k}} \equiv \varepsilon_{\mathbf{k}} + C + \Delta$ with $\varepsilon_{\mathbf{k}} = \hbar^2 \mathbf{k}^2 / (2m)$. By defining collectively $\mathbf{u}_{\mathbf{k}} \equiv [u_{\mathbf{k}1}, u_{\mathbf{k}2}]^T$ and $\mathbf{v}_{\mathbf{k}} \equiv [v_{\mathbf{k}1}, v_{\mathbf{k}2}]^T$, it is easy to check that,

$$\mathbf{u}_{\mathbf{k}} = -\frac{\mathbf{M}}{B_{\mathbf{k}} - E_{\mathbf{k}}} \mathbf{v}_{\mathbf{k}}, \quad (25)$$

$$\mathbf{v}_{\mathbf{k}} = -\frac{\mathbf{M}}{B_{\mathbf{k}} + E_{\mathbf{k}}} \mathbf{u}_{\mathbf{k}}, \quad (26)$$

where

$$\mathbf{M} = \begin{bmatrix} C & -\Delta \\ -\Delta & C \end{bmatrix} \quad (27)$$

is a 2 by 2 matrix. It is straightforward to show that the quasi-particle wave-functions satisfy [37],

$$u_{\mathbf{k}1}^2 = u_{\mathbf{k}2}^2 = \frac{1}{4} \left(\frac{B_{\mathbf{k}}}{E_{\mathbf{k}}} + 1 \right), \quad (28)$$

$$v_{\mathbf{k}1}^2 = v_{\mathbf{k}2}^2 = \frac{1}{4} \left(\frac{B_{\mathbf{k}}}{E_{\mathbf{k}}} - 1 \right), \quad (29)$$

where the dispersion relation $E_{\mathbf{k}}$ can take two branches,

$$E_{\mathbf{k}-} = \sqrt{\varepsilon_{\mathbf{k}} (\varepsilon_{\mathbf{k}} + 2C + 2\Delta)}, \quad (30)$$

$$E_{\mathbf{k}+} = \sqrt{(\varepsilon_{\mathbf{k}} + 2C) (\varepsilon_{\mathbf{k}} + 2\Delta)}. \quad (31)$$

$E_{\mathbf{k}-}$ is the gapless phonon spectrum, while $E_{\mathbf{k}+}$ becomes gapped due to the bosonic pairing. As a result of $E_{\mathbf{k}}(v_{\mathbf{k}1}^2 + v_{\mathbf{k}2}^2) = (B_{\mathbf{k}} - E_{\mathbf{k}})/2$, we obtain from Eq. (15) and Eq. (18) the thermodynamic potential at finite temperature,

$$\Omega = \Omega_0 + \Omega_T, \quad (32)$$

$$\Omega_0 = -\mathcal{V} \left[\frac{C^2}{g} + \frac{\Delta^2}{g_{12}} \right] + \sum_{\mathbf{k}} \left[\frac{E_{\mathbf{k}-} + E_{\mathbf{k}+}}{2} - B_{\mathbf{k}} \right] \quad (33)$$

$$\Omega_T = \frac{1}{\beta} \sum_{\mathbf{k}} \left[\ln(1 - e^{-\beta E_{\mathbf{k}-}}) + \ln(1 - e^{-\beta E_{\mathbf{k}+}}) \right]. \quad (34)$$

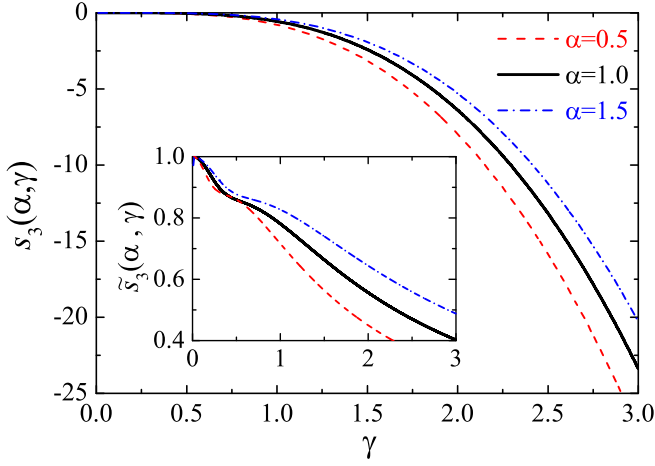


FIG. 1. The function $s_3(\alpha, \gamma)$ as a function of the reduced temperature $\gamma = k_B T/C$ at three different ratios $\alpha = \Delta/C = 0.5$ (red dashed line), 1.0 (black solid line), and 1.5 (blue dot-dashed line). The inset shows the function $\tilde{s}_3(\alpha, \gamma)$.

The quantum and thermal depletions are given by,

$$n_{\text{qd}} = \frac{1}{\mathcal{V}} \sum_{\mathbf{k}} \left[\frac{B_{\mathbf{k}}}{2E_{\mathbf{k}-}} + \frac{B_{\mathbf{k}}}{2E_{\mathbf{k}+}} - 1 \right], \quad (35)$$

$$n_{\text{th}} = \frac{1}{\mathcal{V}} \sum_{\mathbf{k}} \left[\frac{B_{\mathbf{k}}}{E_{\mathbf{k}-}} f_B(E_{\mathbf{k}-}) + \frac{B_{\mathbf{k}}}{E_{\mathbf{k}+}} f_B(E_{\mathbf{k}+}) \right], \quad (36)$$

respectively.

III. THREE-DIMENSIONAL DROPLETS

In three dimensions, the zero-temperature thermodynamic potential Eq. (33) has been discussed in detail in the previous works [35, 36]. By replacing the bare interaction strengths g and g_{12} with the s -wave scattering lengths a and a_{12} , one obtains [35, 36],

$$\frac{\Omega_0}{\mathcal{V}} = -\frac{m}{4\pi\hbar^2} \left[\frac{C^2}{a} + \frac{\Delta^2}{a_{12}} \right] + \frac{8m^{3/2}C^{5/2}}{15\pi^2\hbar^3} \mathcal{G}_3 \left(\frac{\Delta}{C} \right), \quad (37)$$

where $\mathcal{G}_3(\alpha) \equiv (1 + \alpha)^{5/2} + h_3(\alpha)$ with $h_3(\alpha) \equiv (15/4) \int_0^\infty dt \sqrt{t} [\sqrt{(t+1)(t+\alpha)} - (t+1/2 + \alpha/2) + (1 - \alpha)^2/(8t)]$. To carry out the momentum integration in the finite-temperature contribution to the thermodynamic potential Eq. (34), we introduce $t = [\hbar^2 k^2/(2m)]/(2C)$, $\alpha = \Delta/C$ and $\gamma = k_B T/C$ to write the two dispersion relations into the dimensionless forms,

$$\tilde{E}_-(t) = \beta E_{\mathbf{k}-} = \frac{2\sqrt{t(t+1+\alpha)}}{\gamma}, \quad (38)$$

$$\tilde{E}_+(t) = \beta E_{\mathbf{k}+} = \frac{2\sqrt{(t+1)(t+\alpha)}}{\gamma}. \quad (39)$$

Hence, we find that,

$$\frac{\Omega_T}{\mathcal{V}} = \frac{8m^{3/2}C^{5/2}}{15\pi^2\hbar^3} s_3(\alpha, \gamma), \quad (40)$$

where

$$s_3(\alpha, \gamma) \equiv \frac{15}{4} \gamma \int_0^\infty dt \sqrt{t} \sum_{\pm} \ln \left[1 - e^{-\tilde{E}_{\pm}(t)} \right]. \quad (41)$$

At very low temperature, i.e., $k_B T \ll C$ or $\gamma \ll 1$, where the gapless phonon spectrum can be well-approximated as $\tilde{E}_-(t) \simeq (2\sqrt{1+\alpha}/\gamma)\sqrt{t}$ and the gapped mode $\tilde{E}_+(t)$ does not contribute to the integral, we obtain the low-temperature result,

$$\begin{aligned} s_3 &\simeq \frac{15}{4} \gamma \int_0^\infty dt \sqrt{t} \ln \left[1 - \exp \left(-\frac{2\sqrt{1+\alpha}}{\gamma} \sqrt{t} \right) \right], \\ &= -\frac{\pi^4}{48} \frac{\gamma^4}{(1+\alpha)^{3/2}} \propto -T^4. \end{aligned} \quad (42)$$

where in the last step, we have introduced the variable $x = (2\sqrt{1+\alpha}/\gamma)\sqrt{t}$ and have used the identity $\int_0^\infty dx x^2 \ln(1 - e^{-x}) = -\pi^4/45$. Therefore, it is useful to rewrite $s_3(\alpha, \gamma)$ into the form,

$$s_3(\alpha, \gamma) = -\frac{\pi^4}{48} \frac{\gamma^4}{(1+\alpha)^{3/2}} \tilde{s}_3(\alpha, \gamma), \quad (43)$$

where the function $\tilde{s}_3(\alpha, \gamma)$ accounts for the high-order correction at nonzero temperature.

In Fig. 1, we show the functions $s_3(\alpha, \gamma)$ and $\tilde{s}_3(\alpha, \gamma)$ as a function of the reduced temperature γ at three typical ratios $\alpha = \Delta/C = 0.5$ (red dashed line), 1.0 (black solid line), and 1.5 (blue dot-dashed line). We find that $s_3(\alpha, \gamma)$ follows closely its low-temperature approximate result Eq. (42) up to $k_B T \sim C$, i.e., when the thermal energy $k_B T$ becomes comparable to the intraspecies interaction energy C . At this temperature scale, $s_3(\alpha, \gamma) \sim -\mathcal{O}(1)$ is at the same order of the function $\mathcal{G}_3(\alpha)$ but has an opposite sign, indicating that the repulsive force provided by LHY quantum fluctuations might be compensated by thermal fluctuations. More quantitatively, at $\alpha = 1$ where $\mathcal{G}_3(\alpha = 1) = 4\sqrt{2}$, the combined contribution to the thermodynamic potential from quantum and thermal fluctuations,

$$\frac{\Omega_{\text{LHY}}}{\mathcal{V}} = \frac{32\sqrt{2}m^{3/2}C^{5/2}}{15\pi^2\hbar^3} \left[1 - \frac{\pi^4}{768} \gamma^4 \tilde{s}_3(1, \gamma) \right], \quad (44)$$

vanishes at about $\gamma \simeq 2$.

A. Equation of state

For a given chemical potential μ , we numerically calculate the thermodynamic potential $\Omega = \Omega_0 + \Omega_T$ as a function of the pairing gap Δ , by using Eq. (37), Eq. (40) and Eq. (43). The saddle-point solution $\Delta = \Delta_0$ is then obtained by minimizing the thermodynamic potential. After the calculation of the number of particles $N = -\partial\Omega/\partial\mu$, we finally determine the free energy $F = \Omega + \mu N$ and the pressure $P = -\Omega/\mathcal{V}$.

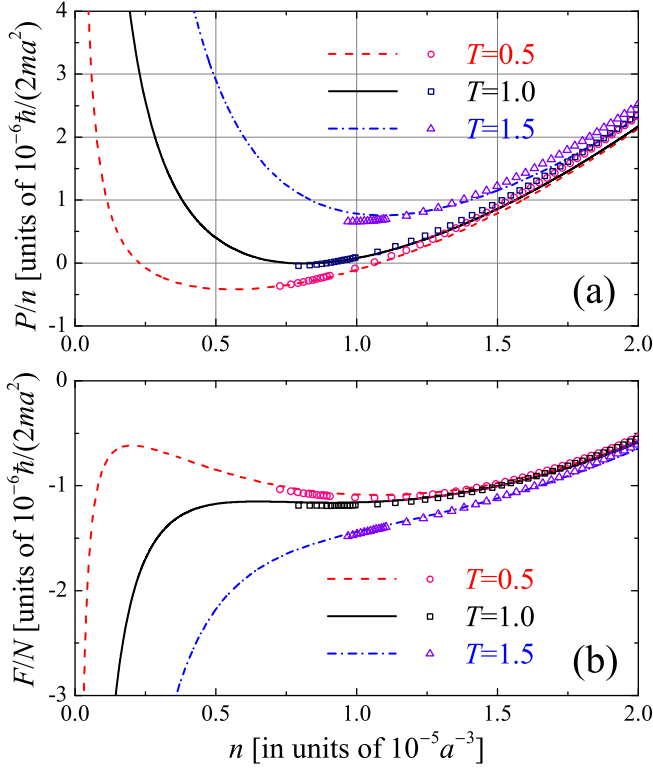


FIG. 2. Pressure per particle P/n (a) and free energy per particle F/N (b) of a 3D droplet, in units of $10^{-6}\hbar^2/(2ma^2)$, as a function of the density n at three temperatures $k_B T = 0.5, 1.0$ and 1.5 measured in units of $10^{-4}\hbar^2/(2ma^2)$. The symbols and lines show the numerical and analytical results, respectively. The density n is in units of $10^{-5}a^{-3}$. We take the inter-species interaction strength $a_{12} = -1.05a$.

Quite generally, in three dimensions the saddle-point pairing gap is much larger than the chemical potential $\Delta_0 \gg |\mu|$ and hence $C = \mu + \Delta_0 \gg |\mu|$ [35, 36]. Therefore, to a very good approximation, around the saddle point ($\Delta \sim \Delta_0$) we obtain,

$$\frac{\Omega}{\mathcal{V}} = -\frac{m\Delta}{2\pi\hbar^2 a}\mu - \frac{m}{4\pi\hbar^2 a}\left(1 + \frac{a}{a_{12}}\right)\Delta^2 + \frac{32\sqrt{2}m^{3/2}\Delta^{5/2}}{15\pi^2\hbar^3}\left[1 - \frac{\pi^4}{768}\gamma^4\tilde{s}_3(1,\gamma)\right], \quad (45)$$

where we have set $C = \Delta$ in the LHY term (i.e., the second line) and thereby $\gamma = k_B T/\Delta$. By taking the derivatives with respect to the chemical potential μ and the pairing gap Δ , i.e., $n = N/\mathcal{V} = -\partial(\Omega/\mathcal{V})/\partial\mu$ and $\partial\Omega/\partial\Delta = 0$ at $\Delta = \Delta_0$, we find that,

$$\Delta_0 = \frac{2\pi\hbar^2 a}{m}n \quad (46)$$

and

$$\mu = -\left(1 + \frac{a}{a_{12}}\right)\Delta_0 + \frac{32\sqrt{2}ma}{3\pi\hbar}\Delta_0^{3/2}\left\{1 + \frac{\pi^4}{1280}\left[\gamma^4\tilde{s}_3(1,\gamma) + \frac{2}{3}\gamma^5\frac{\partial\tilde{s}_3(1,\gamma)}{\partial\gamma}\right]\right\}, \quad (47)$$

respectively. It is then straightforward to obtain the analytic expressions for the pressure P and the free energy F ,

$$P = -\frac{\pi\hbar^2}{m}\left(a + \frac{a^2}{a_{12}}\right)n^2 + \frac{128\sqrt{\pi}}{5}\left(\frac{\hbar^2 a^{5/2}}{m}\right)n^{5/2}\left\{1 + \frac{5\pi^4}{2304}\left[\gamma^4\tilde{s}_3(1,\gamma) + \frac{2}{5}\gamma^5\frac{\partial\tilde{s}_3(1,\gamma)}{\partial\gamma}\right]\right\}, \quad (48)$$

$$\frac{F}{\mathcal{V}} = -\frac{\pi\hbar^2}{m}\left(a + \frac{a^2}{a_{12}}\right)n^2 + \frac{256\sqrt{\pi}}{15}\left(\frac{\hbar^2 a^{5/2}}{m}\right)n^{5/2}\left[1 - \frac{\pi^4}{768}\gamma^4\tilde{s}_3(1,\gamma)\right], \quad (49)$$

where the parameter γ should now be understood as,

$$\gamma = \frac{mk_B T}{2\pi\hbar^2 a n} = \frac{1}{(na^3)^{1/3}[\zeta(3/2)]^{2/3}}\left(\frac{T}{T_c}\right). \quad (50)$$

In the second step of the above equation, we have re-expressed the density n in terms of the small gas parameter $na^3 \ll 1$ and the Bose-Einstein condensation temperature of an ideal gas $k_B T_c = 2\pi\hbar^2[n/(2\zeta(3/2))]^{3/2}/m$, where $\zeta(3/2) \simeq 2.6124$ is the Riemann zeta function. In the zero-temperature limit, the free energy Eq. (49) re-

covers the analytical expression for the ground-state energy found in earlier works [35, 36].

In Fig. 2, we report the numerical and analytical results of the pressure per particle $P/n = -\Omega/N$ (a) and the free energy per particle F/N (b) as a function of the density n , at the inter-species interaction strength $a_{12} = -1.05a$ and at three typical temperatures $k_B T = 0.5, 1.0$ and 1.5 , measured in units of $10^{-4}\hbar^2/(2ma^2)$. There is an excellent agreement between numerical and analytical predictions, as we anticipate. At finite temperature, we find that the density depen-

dence of the pressure and free energy develop non-trivial features in the low-density limit ($n \rightarrow 0$). Instead of becoming vanishingly small as in the zero-temperature case, both equations of state become divergent when the density decreases to zero. This divergence is purely a temperature effect and can be easily understood from the last term in Eq. (48) and Eq. (49), i.e.,

$$\delta P, \delta F \propto n^{5/2} \gamma^4 = n^{5/2} \left(\frac{mk_B T}{2\pi \hbar^2 a n} \right)^4 \sim \frac{T^4}{n^{3/2}}. \quad (51)$$

The temperature correction in the pressure and free energy therefore diverges like $\pm n^{-3/2}$ as the density approaches zero and vanishes like T^4 with decreasing temperature.

As a consequence of such a divergent low-density dependence, at low temperature (i.e., at $k_B T = 0.5 \times 10^{-4} \hbar^2 / (2ma^2)$ as indicated by the red dashed line) we find there are two solutions for the self-bound condition $P = 0$, which correspond to a local maximum and a local minimum in the free energy, respectively. However, the lower density self-bound solution (i.e., the local maximum in the free energy) is not mechanically stable and should be discarded, since one can readily identify that its inverse compressibility,

$$\kappa^{-1} = -\mathcal{V} \left(\frac{\partial P}{\partial \mathcal{V}} \right)_N = n \frac{\partial P}{\partial n} < 0, \quad (52)$$

becomes negative so the system collapses. As we increase temperature, we observe that the two self-bound solutions start to merge and eventually disappear at a threshold temperature $k_B T_{\text{th}} \sim 10^{-4} \hbar^2 / (2ma^2)$. Above this threshold temperature, the pressure is always positive and there is no longer a local minimum in the free energy (see, i.e., the blue dot-dashed lines at $k_B T = 1.5 \times 10^{-4} \hbar^2 / (2ma^2)$). Thus, the self-bound droplet state is completely destabilized by the temperature effect.

B. Threshold temperature for destabilization

We may determine the threshold temperature for destabilization from the analytic expression for the pressure. By setting $P = 0$ in Eq. (48) and using Eq. (50), we obtain that

$$k_B T = \frac{25\pi^2}{8192} \left(1 + \frac{a}{a_{12}} \right)^2 \frac{\hbar^2}{ma^2} f_3(\gamma), \quad (53)$$

where we have defined the function,

$$f_3(\gamma) \equiv \gamma \left\{ 1 + \frac{5\pi^4}{2304} \left[\gamma^4 \tilde{s}_3(1, \gamma) + \frac{2}{5} \gamma^5 \frac{\partial \tilde{s}_3(1, \gamma)}{\partial \gamma} \right] \right\}^{-2}. \quad (54)$$

As shown in the inset of Fig. 3(a), $f_3(\gamma)$ is a non-monotonous function and reaches its maximum

$$\max_{\gamma} [f_3(\gamma)] \simeq 0.7372 \quad (55)$$

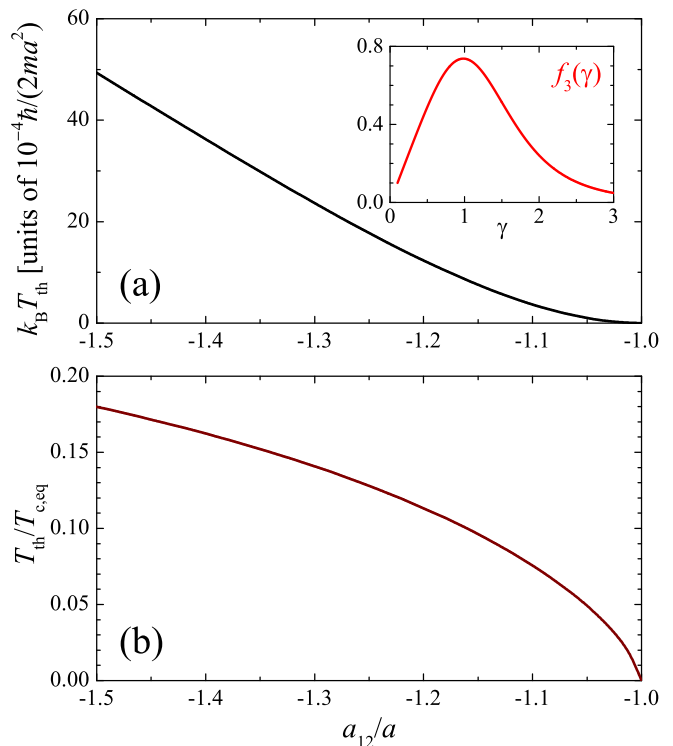


FIG. 3. Threshold temperature T_{th} of a 3D droplet as a function of the inter-species interaction strength a_{12}/a , measured in units of $10^{-4} \hbar^2 / (2ma^2)$ (a) and in units of the ideal gas BEC transition temperature $T_{c,\text{eq}}$ at the zero-temperature equilibrium density n_{eq} (b), as predicted by the analytic equation (58). The inset in (a) show the function $f_3(\gamma)$.

at $\gamma_{\text{th}} \simeq 0.9835$. Therefore, we find

$$k_B T_{\text{th}} \simeq 0.0222 \left(1 + \frac{a}{a_{12}} \right)^2 \frac{\hbar^2}{ma^2}, \quad (56)$$

which is shown in Fig. 3(a) as a function of the interaction strength ratio a_{12}/a . By recalling that the zero-temperature equilibrium density n_{eq} is given by [35],

$$n_{\text{eq}} = \frac{25\pi}{16384} \left(1 + \frac{a}{a_{12}} \right)^2 a^{-3}, \quad (57)$$

we can measure the threshold temperature in units of the condensation temperature $T_{c,\text{eq}}$ at the equilibrium density n_{eq} ,

$$\frac{T_{\text{th}}}{T_{c,\text{eq}}} \simeq 0.3742 \left(1 + \frac{a}{a_{12}} \right)^{2/3}. \quad (58)$$

As can be seen from Fig. 3(b), under the typical experimental conditions (i.e., $a_{12} \sim [-1.10, -1.05]a$ as in Refs. [9, 11]), the threshold temperature is less than one-tenth of the condensation temperature. This small threshold temperature can alternatively be understood from Eq. (50). At the threshold reduced temperature, $\gamma_{\text{th}} \sim 1$, we

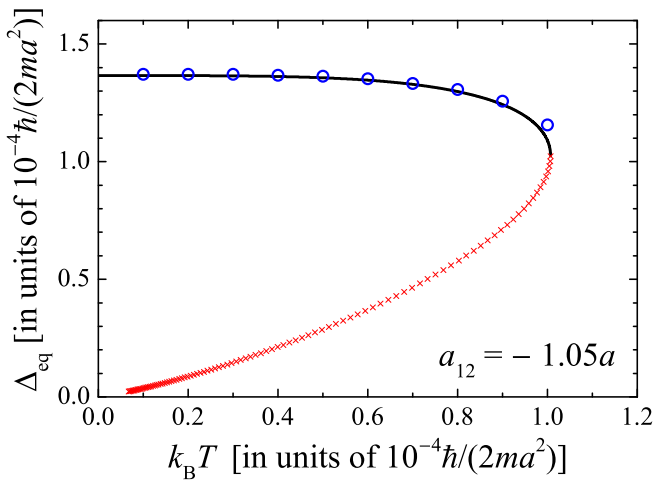


FIG. 4. Temperature dependence of the equilibrium pairing gap Δ_{eq} of a 3D droplet at the inter-species interaction strength $a_{12} = -1.05a$. The equilibrium pairing gap Δ_{eq} and temperature $k_B T$ are both measured in units of $10^{-4}\hbar^2/(2ma^2)$. The blue circles and black line show the numerical and analytical results, respectively. The red crosses correspond to the unphysical solution, in which the droplet becomes mechanically unstable with $\partial P/\partial n < 0$.

find that $T_{\text{th}}/T_{c,\text{eq}} \sim (na^3)^{1/3} \sim 0.1$ for the small interaction parameter $na^3 \sim 10^{-5} - 10^{-4}$ in the experiments [9, 11].

In Fig. 4, we present the temperature dependence of the equilibrium pairing parameter $\Delta_{\text{eq}}(T)$ at the inter-species interaction strength $a_{12} = -1.05a$. As the pairing parameter is proportional to the density, this figure also shows the equilibrium density n_{eq} as a function of temperature. In general, with increasing temperature there are two branches in $\Delta_{\text{eq}}(T)$ and $n_{\text{eq}}(T)$. The lower branch, which is shown by red crosses, corresponds to the unstable low-density self-bound solution we discussed earlier and therefore should be neglected. We find that for $T < 0.7T_{\text{th}}$ the temperature dependence in the upper branch n_{eq} is relatively weak. However, towards and upon reaching the threshold temperature, the equilibrium density n_{eq} can decrease significantly, by several tens of percent in relative.

C. Quantum and thermal depletions

The results we presented so far are all obtained within the Bogoliubov theory, which is valid at sufficiently low temperature in the weakly interacting regime. To have a self-consistent check, in Fig. 5, we show the quantum depletion (a) and thermal depletion (b) as a function of the density at the inter-species interaction strength $a_{12} = -1.05a$, obtained by using Eq. (35) and Eq. (36). At the typical temperatures considered in this figure, the quantum depletion is less than one percent and is essentially temperature dependent. The thermal depletion

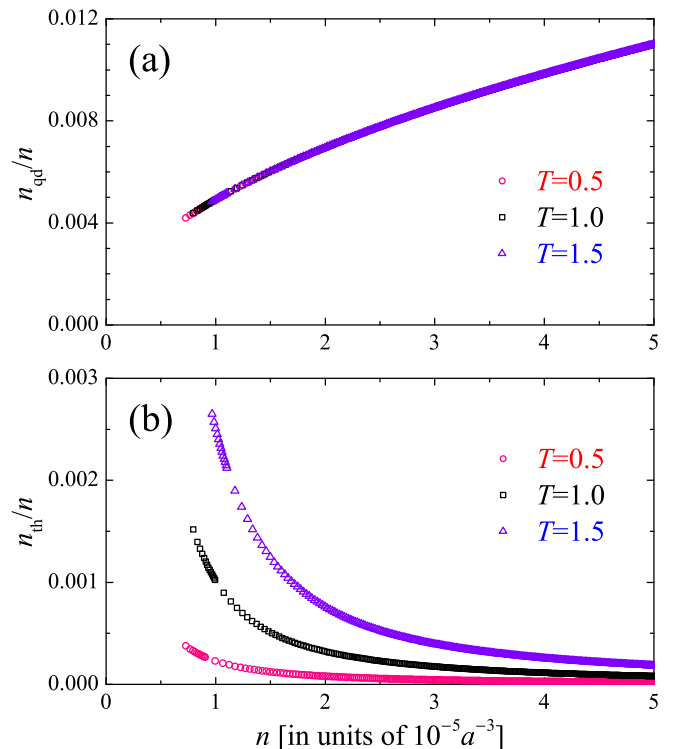


FIG. 5. Quantum depletions (a) and thermal depletions (b) of a 3D droplet as a function of the density n (in units of $10^{-5}a^{-3}$) at the inter-species interaction strength $a_{12} = -1.05a$. We consider three temperatures $k_B T = 0.5, 1.0$ and 1.5 , measured in units of $10^{-4}\hbar^2/(2ma^2)$.

is even smaller and is about 0.1% close to the threshold temperature for the thermal destabilization of the droplet state. Therefore, we conclude that the conditions for the application of the Bogoliubov theory are well satisfied.

IV. ONE-DIMENSIONAL DROPLETS

We now turn to consider one-dimensional quantum droplets. In this case, counterintuitively, the droplet formation is driven by LHY quantum fluctuations [18, 28], which provide an attractive force to the system. It is then balanced by the repulsive mean-field force under the condition $g > -g_{12}$. As given in our earlier work [36], the zero-temperature thermodynamic potential takes the form (\mathcal{V} is now the length of the system),

$$\frac{\Omega_0}{\mathcal{V}} = - \left[\frac{C^2}{g} + \frac{\Delta^2}{g_{12}} \right] - \frac{2\sqrt{m}}{3\pi\hbar} C^{3/2} \mathcal{G}_1 \left(\frac{\Delta}{C} \right), \quad (59)$$

where $\mathcal{G}_1(\alpha) \equiv (1 + \alpha)^{3/2} + h_1(\alpha)$ with $h_1 \equiv (3/2) \int_0^\infty dt t^{-1/2} [t + (1 + \alpha)/2 - \sqrt{(t+1)(t+\alpha)}]$. As in the three-dimensional case, we introduce the variables t , α and γ to rewrite the finite-temperature contribution

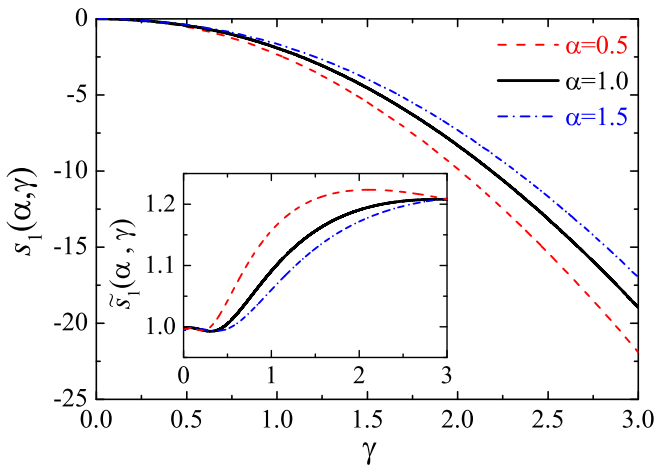


FIG. 6. The function $s_1(\alpha, \gamma)$ as a function of the reduced temperature $\gamma = k_B T/C$ at three different ratios $\alpha = \Delta/C = 0.5$ (red dashed line), 1.0 (black solid line), and 1.5 (blue dot-dashed line). The inset shows the function $\tilde{s}_1(\alpha, \gamma)$.

to the thermodynamic potential,

$$\frac{\Omega_T}{\mathcal{V}} = \frac{2\sqrt{m}}{3\pi\hbar} C^{3/2} s_1(\alpha, \gamma), \quad (60)$$

where

$$s_1(\alpha, \gamma) \equiv \frac{3}{2}\gamma \int_0^\infty dt \frac{1}{\sqrt{t}} \sum_{\pm} \ln \left[1 - e^{-\tilde{E}_{\pm}(t)} \right]. \quad (61)$$

At very low temperature $\gamma \ll 1$, where only the gapless phonon mode contributes to the integral for $s_1(\alpha, \gamma)$, we obtain,

$$s_1 \simeq 3\gamma \int_0^\infty dt \ln \left(1 - e^{-2t\sqrt{1+\alpha}/\gamma} \right) = -\frac{\pi^2 \gamma^2}{4\sqrt{1+\alpha}}. \quad (62)$$

Therefore, it is convenient to rewrite $s_1(\alpha, \gamma)$ in the form,

$$s_1(\alpha, \gamma) = -\frac{\pi^2}{4} \frac{\gamma^2}{\sqrt{1+\alpha}} \tilde{s}_1(\alpha, \gamma). \quad (63)$$

The temperature- or γ -dependence of $s_1(\alpha, \gamma)$ and $\tilde{s}_1(\alpha, \gamma)$ at three selected values of α is shown in Fig. 6. In contrast to the three-dimensional case, we find that the higher-order correction factor \tilde{s}_1 is generally larger than 1.0 and does not change too significantly as we increase the temperature.

By collecting the contributions from quantum and thermal fluctuations to the thermodynamic potential, we obtain ($\alpha = C/\Delta$ and $\gamma = k_B T/C$),

$$\frac{\Omega_{\text{LHY}}}{\mathcal{V}} = -\frac{2\sqrt{m}}{3\pi\hbar} C^{3/2} \left[\mathcal{G}_1(\alpha) + \frac{\pi^2 \gamma^2}{4\sqrt{1+\alpha}} \tilde{s}_1(\alpha, \gamma) \right]. \quad (64)$$

It is clear that the contributions from quantum and thermal fluctuations do not cancel with each other and

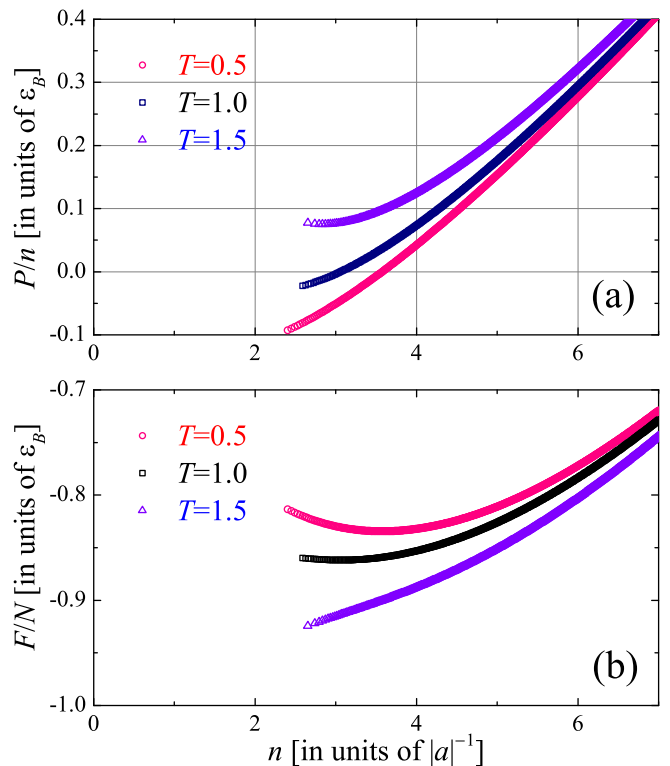


FIG. 7. Pressure per particle P/n (a) and free energy per particle F/N (b) of a 1D droplet, in units of ε_B , as a function of the density n (in units of $|a|^{-1}$) at three temperatures $k_B T/\varepsilon_B = 0.5, 1.0$ and 1.5 and at the inter-species interaction strength $g_{12} = -0.75g$. The pressure and free energy per particle and temperature are all measured in units of $\varepsilon_B = \hbar^2/(ma_{12}^2)$.

become comparable at the reduced temperature $\gamma \sim \mathcal{O}(1)$. Naively, one may think that thermal fluctuations enhance the stability of the the one-dimensional droplet state, contrary to its three-dimensional counterpart. However, it turns out to be an incorrect picture.

We have performed numerical calculations for the equations of state, by minimizing $\Omega = \Omega_0 + \Omega_T$ in Eq. (59) and Eq. (60) at a given chemical potential μ and consequently calculating the pressure and the free energy. Their numerical results at the inter-species interaction strength $g_{12} = -0.75g$ is reported in Fig. 7. As shown in (a) for pressure, at sufficiently low temperature, i.e., $k_B T = 0.5\varepsilon_B$, where $\varepsilon_B = \hbar^2/(ma_{12}^2)$ is the binding energy for an inter-species dimer, we find a droplet state satisfying the self-bound condition $P = 0$ (or equivalently a local minimum F/N) at the density $n_{\text{eq}} \sim 3|a|^{-1}$. With increasing temperature ($k_B T = \varepsilon_B$), the equilibrium density n_{eq} becomes smaller. At the largest temperature considered in the figure, i.e., $k_B T = 1.5\varepsilon_B$, it seems that the pressure P is always positive and at the same time the free energy per particle decreases monotonically as the density decreases to zero. Therefore, the self-bound droplet state disappears at a threshold temperature $\varepsilon_B < k_B T_{\text{th}} < 1.5\varepsilon_B$.

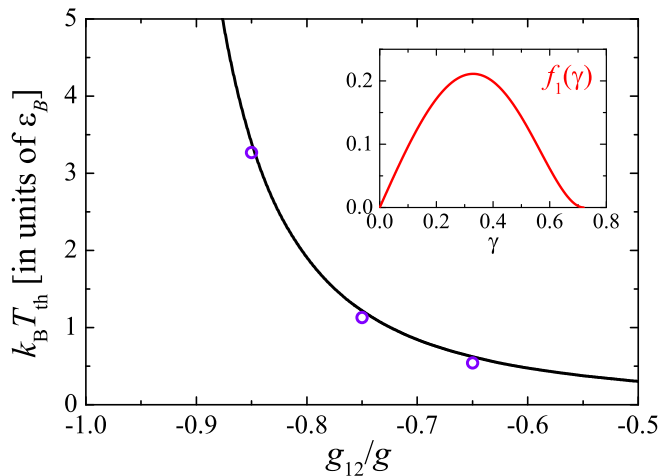


FIG. 8. Threshold temperature T_{th} (in units of ε_B) of a 1D droplet as a function of the inter-species interaction strength g_{12}/g , predicted by the analytic equation (69). The empty circles report the results from numerical calculations. The inset shows the function $f_1(\gamma)$.

To understand the thermal destabilization of the droplet state, it is useful to derive an analytic expression for the pressure, following the same steps in the three-dimensional case. However, we note that, the condition $|\mu| \ll C$, Δ_0 is not so well-satisfied in one dimension [36]. As a result, the analytic expressions derived are of qualitative use only (so we do not show them in Fig. 7). For the pressure P , it is straightforward to obtain that,

$$P = -\frac{1}{4} \left(g + \frac{g^2}{g_{12}} \right) n^2 - \frac{\sqrt{m}g^{3/2}}{3\pi\hbar} n^{3/2} + \frac{\pi\sqrt{m}g^{3/2}}{16\hbar} n^{3/2} \left[\gamma^2 \tilde{s}_1(1, \gamma) + \frac{2}{3} \gamma^3 \frac{\partial \tilde{s}_1(1, \gamma)}{\partial \gamma} \right] \quad (65)$$

where the last two terms come from quantum fluctuations and thermal fluctuations, respectively. It is easy to see that, while the contribution from quantum fluctuations to the pressure is negative, the contribution from thermal fluctuations is always positive and increases with increasing temperature, consistent with our numerical results shown in Fig. 7(a). Therefore, thermal fluctuations eventually destroy the droplet state.

By setting $P = 0$ in Eq. (65), we find the relation,

$$k_B T = \frac{32}{9\pi^2} \frac{\varepsilon_B}{(1 + g_{12}/g)^2} f_1(\gamma), \quad (66)$$

where

$$f_1(\gamma) \equiv \gamma \left\{ 1 - \frac{3\pi^2}{16} \left[\gamma^2 \tilde{s}_1(1, \gamma) + \frac{2}{3} \gamma^3 \frac{\partial \tilde{s}_1(1, \gamma)}{\partial \gamma} \right] \right\}^2. \quad (67)$$

The function $f_1(\gamma)$ is shown in the inset of Fig. 8. There is a maximum

$$\max_{\gamma} [f_1(\gamma)] \simeq 0.21116 \quad (68)$$

at $\gamma_{\text{th}} \simeq 0.330$. Therefore, the threshold temperature in one dimension is given by,

$$k_B T_{\text{th}} \simeq 0.0761 \frac{\varepsilon_B}{(1 + g_{12}/g)^2}. \quad (69)$$

This analytical prediction is shown in Fig. 8 by using a black solid line. We have also numerically determined the threshold temperature by repeating the calculations in Fig. 7 at different inter-species interaction strengths and show the results in the figure by empty circles. It seems that there is a good agreement between numerical and analytical results. In the interval of interest, i.e., $g_{12} \sim [-0.9, -0.5]g$, the threshold temperature is roughly at the order of the binding energy ε_B of the inter-species dimer.

V. CONCLUSIONS

In summary, we have presented a systematic investigation of the temperature effect in self-bound ultradilute quantum droplets, both in three dimensions and in one dimension, by extending a recently developed microscopic pairing theory [35, 36] to nonzero temperature. We have shown that thermal fluctuations generally destabilize the droplet state and destroy it above a threshold temperature. The energy scale of the threshold temperature is at the order of the intra-species interaction energy and is therefore very small in the weakly interacting regime. For a three-dimensional quantum droplet, the threshold temperature is less than one-tenth of the Bose-Einstein condensation temperature under current experimental conditions [9, 11]. We have also predicted the temperature dependence of the equilibrium density and have found that it can decrease by several tens of percent upon reaching the threshold temperature.

Our predictions could be readily examined in future experiments on quantum droplets realized by a binary Bose mixture with attractive inter-species interactions. The sensitive temperature dependence of the droplet state may alternatively provide us good thermometry in ultracold atomic experiments, where the low temperature at the scale of one-tenth of the condensation temperature is often challenging to measure.

ACKNOWLEDGMENTS

This research was supported by the Australian Research Council's (ARC) Discovery Program, Grants No. DE180100592 and No. DP190100815 (J.W.), Grant No. DP170104008 (H.H.), and Grant No. DP180102018 (X.-J.L.).

-
- [1] G. E. Volovik, *The Universe in a Helium Droplet*, page 27-29 (Oxford University Press, Cambridge, 2009).
- [2] J. Harms, J. P. Toennies, and F. Dalfovo, Density of superfluid helium droplets, *Phys. Rev. B* **58**, 3341 (1998).
- [3] M. Barranco, R. Guardiola, S. Hernández, R. Mayol, J. Navarro, and M. Pi, Helium Nanodroplets: an Overview, *J. Low Temp. Phys.* **142**, 1 (2006).
- [4] O. Gessner and A. F. Vilesov, Imaging Quantum Vortices in Superfluid Helium Droplets, *Annu. Rev. Phys. Chem.* **70**, 173 (2019).
- [5] F. Dalfovo, S. Giorgini, L. P. Pitaevskii, and S. Stringari, Theory of Bose-Einstein condensation in trapped gases, *Rev. Mod. Phys.* **71**, 463 (1999).
- [6] E. A. Donley, N. R. Claussen, S. L. Cornish, J. L. Roberts, E. A. Cornell, and C. E. Wieman, Dynamics of collapsing and exploding Bose-Einstein condensates, *Nature (London)* **412**, 295 (2001).
- [7] D. S. Petrov, Quantum Mechanical Stabilization of a Collapsing Bose-Bose Mixture, *Phys. Rev. Lett.* **115**, 155302 (2015).
- [8] T. D. Lee, K. Huang, and C. N. Yang, Eigenvalues and Eigenfunctions of a Bose System of Hard Spheres and Its Low-Temperature Properties, *Phys. Rev.* **106**, 1135 (1957).
- [9] C. Cabrera, L. Tanzi, J. Sanz, B. Naylor, P. Thomas, P. Cheiney, and L. Tarruell, Quantum liquid droplets in a mixture of Bose-Einstein condensates, *Science* **359**, 301 (2018).
- [10] P. Cheiney, C. R. Cabrera, J. Sanz, B. Naylor, L. Tanzi, and L. Tarruell, Bright Soliton to Quantum Droplet Transition in a Mixture of Bose-Einstein Condensates, *Phys. Rev. Lett.* **120**, 135301 (2018).
- [11] G. Semeghini, G. Ferioli, L. Masi, C. Mazzinghi, L. Wolswijk, F. Minardi, M. Modugno, G. Modugno, M. Inguscio, and M. Fattori, Self-Bound Quantum Droplets of Atomic Mixtures in Free Space, *Phys. Rev. Lett.* **120**, 235301 (2018).
- [12] G. Ferioli, G. Semeghini, L. Masi, G. Giusti, G. Modugno, M. Inguscio, A. Gallelli, A. Recati, and M. Fattori, Collisions of Self-Bound Quantum Droplets, *Phys. Rev. Lett.* **122**, 090401 (2019).
- [13] C. D'Errico, A. Burchianti, M. Prevedelli, L. Salasnich, F. Ancilotto, M. Modugno, F. Minardi, and C. Fort, Observation of quantum droplets in a heteronuclear bosonic mixture, *Phys. Rev. Research* **1**, 033155 (2019).
- [14] I. Ferrier-Barbut, H. Kadau, M. Schmitt, M. Wenzel, and T. Pfau, Observation of Quantum Droplets in a Strongly Dipolar Bose Gas, *Phys. Rev. Lett.* **116**, 215301 (2016).
- [15] M. Schmitt, M. Wenzel, F. Böttcher, I. Ferrier-Barbut, and T. Pfau, Self-bound droplets of a dilute magnetic quantum liquid, *Nature (London)* **539**, 259 (2016).
- [16] L. Chomaz, S. Baier, D. Petter, M. J. Mark, F. Wächtler, L. Santos, and F. Ferlaino, Quantum-Fluctuation-Driven Crossover from a Dilute Bose-Einstein Condensate to a Macrodroplet in a Dipolar Quantum Fluid, *Phys. Rev. X* **6**, 041039 (2016).
- [17] F. Böttcher, M. Wenzel, J.-N. Schmidt, M. Guo, T. Langen, I. Ferrier-Barbut, T. Pfau, R. Bombín, J. Sánchez-Baena, J. Boronat, and F. Mazzanti, Dilute dipolar quantum droplets beyond the extended Gross-Pitaevskii equation, *Phys. Rev. Research* **1**, 033088 (2019).
- [18] D. S. Petrov and G. E. Astrakharchik, Ultradilute Low-Dimensional Liquids, *Phys. Rev. Lett.* **117**, 100401 (2016).
- [19] D. Baillie, R. M. Wilson, R. N. Bisset, and P. B. Blakie, Self-bound dipolar droplet: A localized matter wave in free space, *Phys. Rev. A* **94**, 021602(R) (2016).
- [20] F. Wächtler and L. Santos, Ground-state properties and elementary excitations of quantum droplets in dipolar Bose-Einstein condensates, *Phys. Rev. A* **94**, 043618 (2016).
- [21] Y. Li, Z. Luo, Y. Liu, Z. Chen, C. Huang, S. Fu, H. Tan, and B. A. Malomed, Two-dimensional solitons and quantum droplets supported by competing self- and cross-interactions in spin-orbit-coupled condensates, *New J. Phys.* **19**, 113043 (2017).
- [22] A. Cappellaro, T. Macrì, and L. Salasnich, Collective modes across the soliton-droplet crossover in binary Bose mixtures, *Phys. Rev. A* **97**, 053623 (2018).
- [23] Emerson Chiquillo, Equation of state of the one- and three-dimensional Bose-Bose gases, *Phys. Rev. A* **97**, 063605 (2018).
- [24] G. E. Astrakharchik and B. A. Malomed, Dynamics of one-dimensional quantum droplets, *Phys. Rev. A* **98**, 013631 (2018).
- [25] X. Cui, Spin-orbit-coupling-induced quantum droplet in ultracold Bose-Fermi mixtures, *Phys. Rev. A* **98**, 023630 (2018).
- [26] C. Staudinger, F. Mazzanti and R. E. Zillich, Self-bound Bose mixtures, *Phys. Rev. A* **98**, 023633 (2018).
- [27] F. Ancilotto, M. Barranco, M. Guilleumas and M. Pi, *Phys. Rev. A* **98**, 053623 (2018).
- [28] L. Parisi, G. E. Astrakharchik, and S. Giorgini, Liquid State of One-Dimensional Bose Mixtures: A Quantum Monte Carlo Study, *Phys. Rev. Lett.* **122**, 105302 (2019).
- [29] E. Aybar and M. Ö. Oktel, Temperature-dependent density profiles of dipolar droplets, *Phys. Rev. A* **99**, 013620 (2019).
- [30] V. Cikojević, L. Vranješ Markić, G. E. Astrakharchik, and J. Boronat, Universality in ultradilute liquid Bose-Bose mixtures, *Phys. Rev. A* **99**, 023618 (2019).
- [31] Emerson Chiquillo, Low-dimensional self-bound quantum Rabi-coupled bosonic droplets, *Phys. Rev. A* **99**, 051601(R) (2019).
- [32] M. Tylutki, G. E. Astrakharchik, B. A. Malomed, and D. S. Petrov, Collective excitations of a one-dimensional quantum droplet, *Phys. Rev. A* **101**, 051601(R) (2020).
- [33] V. Cikojević, L. Vranješ Markić, and J. Boronat, Finite-range effects in ultradilute quantum drops, *New J. Phys.* **22**, 053045 (2020).
- [34] Y. Wang, L. Guo, S. Yi, and T. Shi, Theory for Self-Bound States of Dipolar Bose-Einstein Condensates, *arXiv:2002.11298* (2020).
- [35] H. Hu and X.-J. Liu, Consistent theory of self-bound quantum droplets with bosonic pairing, *arXiv:2005.08581* (2020).
- [36] H. Hu and X.-J. Liu, Microscopic pairing theory of ultradilute low-dimensional quantum droplets, *arXiv:2006.00434* (2020).
- [37] H. Hu and X.-J. Liu, Microscopic theory of inhomogeneous ultradilute quantum droplets, *arXiv:2006.05769* (2020).

- [38] D. M. Larsen, Binary mixtures of dilute Bose gases with repulsive interactions at low temperature, *Ann. Phys. (N.Y.)* **24**, 89 (1963).
- [39] A. L. Fetter, Nonuniform States of an Imperfect Bose Gas, *Ann. Phys. (N.Y.)* **70**, 67 (1972).
- [40] A. Griffin, Conserving and gapless approximations for an inhomogeneous Bose gas at finite temperatures, *Phys. Rev. B* **53**, 9341 (1996).